A Rapid Numerical Procedure for Determining Axisymmetric Transverse Electric Electromagnetic Fields Via Boundary Integrals

Ira B. Bernstein[†], V. Rokhlin[‡]

Research Report YALEU/DCS/RR-652

September 1988

YALE UNIVERSITY
DEPARTMENT OF COMPUTER SCIENCE

(4)

A method is presented for the rapid efficient determination of axisymmetric transverse electric vacuum electromagnetic fields. The problem is reduced to consideration of boundary integral equations, and these are then solved by perspicuous numerical algorithms. The method has been applied to the cases of the tapered waveguide, the horn, the scatterer, the closed cavity, and the open resonator.

A Rapid Numerical Procedure for Determining Axisymmetric Transverse Electric Electromagnetic Fields Via Boundary Integrals

Ira B. Bernstein†, V. Rokhlin‡

Research Report YALEU/DCS/RR-652

September 1988

† This author was supported in part by the Office of Naval Research under Grant N00014-83-K-0610

‡ This author was supported in part by the Office of Naval Research under Grant N00014-86-K-0310, and in part by IBM under grant P00038437

1-Introduction

An important engineering problem is the determination of the electromagnetic fields in microwave systems, for example tapered waveguides, horns, scatterers, closed cavities, and open resonators. We here consider the case of axisymetric transverse electric modes. Such problems for monochromatic radiation can be reduced to consideration of an elliptic partial differential equation similar to the Helmholtz equation[1]. Methods have been developed for the direct numerical solution of the partial differential equation[1]. Variational principles have been used to optimally determine approximate values of objects of interest like reflection and transmission coefficients[1]. An alternative approach is the reduction of the problem to consideration of an integral equation defined on the metallic walls defining the object[2] (the boundary integral method). These have been solved for the case of scalar fields described by the Helmholtz equation[2]. The boundary integral equation method is feasible when the Greens function is known in a computationaly convenient form, and is very often much more computationaly efficient than its competitors, particularly when the geometry is complex. We here describe the theory and effective numerical implementation of such a boundary integral equation approach for the case of an axisymetric transverse electric electromagnetic field. The technique is readily generalizable to arbitrary axisymmetric fields.

2 - Mathematical and Physical Preliminaries

Consider a transverse electric field which in cylindrical coordinates ρ,ϕ,z can be expressed as

$$\mathbf{E}=(\nabla\phi)\mathrm{Re}\left[e^{-i\omega t}\Psi(\rho,z)\right] \tag{1}$$

Note that $\nabla\phi = \mathbf{e}_\phi/\rho$. The Maxwell equations read for this case

$$\nabla\mathbf{x}\mathbf{E} = i\omega\mu\mathbf{H} \tag{2}$$

$$\nabla\mathbf{x}\mathbf{H} = -i\omega\varepsilon\mathbf{E} \tag{3}$$

where the dielectric constant ε and permeability μ will be taken to have their vacuum values. The situation where they are piecewise constant, appropriate for example for a waveguide with dielectric layers, can readily be treated by a generalization of the methods to be presented. It follows directly from (1) and (2) that

$$\mathbf{H} = -i\frac{(\nabla\Psi)\mathbf{x}\nabla\phi}{\omega\mu} = -i\frac{(\nabla\Psi)\mathbf{x}\mathbf{e}_\phi}{\rho\omega\mu} \tag{4}$$

If one forms the scalar product of (3) with $\nabla\phi$, on using (4) to eliminate H and (2) to express E, there results after some algebra

$$L\{\Psi\} = \nabla\cdot\left(\frac{\nabla\Psi}{\rho^2}\right)+\frac{\omega^2 e\mu\Psi}{\rho^2} = 0 \tag{5}$$

or on writing things out in cylindrical coordinates

$$L\{\Psi\} = \frac{1}{\rho}\frac{\partial}{\partial\rho}\left(\frac{1}{\rho}\frac{\partial\Psi}{\partial\rho}\right)+\frac{\partial}{\partial z}\left(\frac{1}{\rho^2}\frac{\partial\Psi}{\partial z}\right)+\frac{\omega^2 e\mu\Psi}{\rho^2} = 0 \tag{6}$$

The time averaged Poynting vector

$$\Gamma = i\frac{\Psi\nabla\Psi^*-\Psi^*\nabla\Psi}{4\omega\mu\rho^2} \tag{7}$$

and it is readily established from (5) that

$$\nabla\cdot\Gamma = 0 \tag{8}$$

Eq. (7) can conveniently be employed in testing numerical results.

In vacuum $e\mu = 1/c^2$, where c is the speed of light. Define $k=\omega/c$. We shall require for what follows the outgoing Greens function associated with (5). It is, as shown in Appendix A,

$$K(\rho,\rho',z-z') = \rho\rho'\int_0^{2\pi} d\phi\ \frac{e^{ikR}}{4\pi R}\, e^{-i(\phi-\phi')} \tag{9}$$

where, since $\mathbf{r} = \rho\mathbf{e}_\rho+z\mathbf{e}_z$ and $\mathbf{r}' = \rho'\mathbf{e}_\rho+z'\mathbf{e}_z$, the separation

$$R = |\mathbf{r}-\mathbf{r}'| = \left[\rho^2+\rho'^2-2\rho\rho'\cos(\phi-\phi')+(z-z')^2\right]^{1/2} \tag{10}$$

. As is also shown in appendix A

$$L\{K\} = \frac{\delta(\rho-\rho')\delta(z-z')}{(\rho\rho')^{1/2}} \tag{11}$$

Note that K is invariant under interchange of primed and unprimed arguments. Thus

$$L'\{K\} = \frac{1}{\rho'}\frac{\partial}{\partial\rho'}\left(\frac{1}{\rho'}\frac{\partial K}{\partial\rho'}\right)+\frac{\partial}{\partial z'}\left(\frac{1}{\rho'^2}\frac{\partial K}{\partial z'}\right)+\frac{k^2K}{\rho'^2} = -\frac{\delta(\rho-\rho')\delta(z-z')}{(\rho\rho')^{1/2}} \tag{12}$$

The Greens function can be used to reduce the problem of determining Ψ to the solution of an integral equation on the perfectly conducting metallic surfaces assumed to bound the system. This serves to replace the partial differential equation (5), defined on a two dimensional domain, by a problem defined on a one dimensional domain. There are, indeed, a number of such integral equations. We shall deal with one such which is of the second kind and provides a formulation which is numerically stable.

Suppose that the domain of interest is a volume V bounded by a surface S obtained by rotating around the z axis a curve Γ defined in a plane ϕ=const. Let s denote arc length along Γ, and suppose that Γ is defined by the parametric equations $\rho=\rho(s)$ and $z=z(s)$. Then $ds=[(d\rho)^2+(dz)^2]^{1/2}$. The volume element is $d^3r=\rho d\rho d\phi dz$. The vector element of surface is $d^2r=nrdsd\phi$, where $n=n_\rho(\rho,z)e_\rho+n_z(\rho,z)e_z$ is the unit normal pointing out of V. We seek an axisymmetric function $\sigma(\rho,z)$ defined on A such that

$$2\pi\Psi(\rho',z') = \int_A d^2r \cdot \frac{\sigma \nabla K}{\rho} \tag{13}$$

or equivalently

$$\Psi(\rho',z') = \int_\Gamma ds\, \sigma \frac{\partial K}{\partial n} \tag{14}$$

For any point ρ',z' interior to V and not on Γ it follows from (11) and (13) that $L'\{\Psi(\rho',z')\}=0$. But on Γ, as shown in appendix A, because of the singular nature of K as $r\rightarrow r'$, eq. (13) reduces to

$$\phi(s') = \sigma(s') + \int_\Gamma F(s',s)\sigma(s)ds \tag{15}$$

where the inhomogeneous term

$$\phi(s') = \frac{2\Psi(\rho(s'),z(s'))}{\rho(s')} \tag{16}$$

is presumed to be given. The kernel

$$F(s',s) = \mathbf{n}(\rho,z)\cdot\nabla\left[\frac{2K(\rho,\rho',z-z')}{\rho'}\right]_{\rho=\rho(s)\ z=z(s)\ \rho'=\rho(s')\ z'=z(s')} \tag{17}$$

develops a simple pole as $s\to s'$, whence the integral must be interpreted as a Cauchy principal value. The factor

$$\mathbf{n}\cdot\nabla K = \frac{\partial K}{\partial n} = n_\rho(\rho,z)\frac{\partial K(\rho,z;\rho',z')}{\partial \rho} + n_z(\rho,z)\frac{\partial K(\rho,z;\rho',z')}{\partial z} \tag{18}$$

Eq. (15) is the desired integral equation of the second kind for σ.

For the case of horns and scatterers one is concerned with the field far from the object. This is readily determined from the integral representation (13). To this end note that as $r'=(\rho'^2+z'^2)^{1/2}\to\infty$, one has $|\mathbf{r}-\mathbf{r}'| \sim r' - \mathbf{r}\cdot(\mathbf{r}'/r') + \cdots$, whence to lowest significant order in r/r'

$$K \sim \rho\rho'\frac{e^{ikr'}}{4\pi r'}\int_0^{2\pi} d\phi\, \exp\left[-i(\phi-\phi') - ik\,\frac{\rho\rho'\cos(\phi-\phi') + zz'}{r'}\right]$$

$$\sim \rho\rho'\frac{e^{ikr'}}{4\pi r'}2\pi J_1\left(\frac{k\rho\rho'}{r'}\right)\exp\left(-\frac{ikzz'}{r'}\right) \tag{19}$$

On using (14) it is easily established from (1), (13), (17), and (19) that asymptotically as $r'/r\to\infty$

$$E(\rho',z') \sim \frac{e^{ikr'}}{r'}f(\theta') \tag{20}$$

where $\cos\theta'=z'/r'$, and the "scattering amplitude" is

$$f(\theta') = \frac{1}{2}\int_\Gamma \frac{ds}{\rho}\left[n_\rho\left(\frac{\partial\Psi}{\partial\rho} - \Psi\frac{\partial}{\partial\rho}\right) + n_z\left(\frac{\partial\Psi}{\partial z} - \Psi\frac{\partial}{\partial z}\right)\right]$$

$$\left[\exp(-ikz\cos\theta')\right]J_1(k\rho\sin\theta') \tag{21}$$

In the integrand of (19) one must evaluate all the derivatives and then express ρ and z in terms of s.

3-The Tapered Waveguide, Horn, and Scatterer

The configurations with which we shall be concerned are tapered waveguides, cavities (both closed and open), horns, and scatterers. Consider first a tapered perfectly conducting

waveguide as shown schematically in fig 1 . The metallic wall indicated by the heavy line is assumed to have an assigned thickness and shape. The sections on the far right and left are supposed to be long straight sections of constant radius R_+ on the right and R_- on the left. They are joined by a tapered section the radius of which is $R = R(z)$. The system is taken to be enclosed by metallic walls which are assumed to be ideally conducting. This requires that the tangential component of the electrical field vanish on the walls, whence, following (1), $\Psi=0$ on the walls.

For an infinite cylindrical waveguide of radius $R_\pm$, as can be readily determined by separation of variables, eq. (15) has eigensolutions

$$F_n\left(\frac{\rho}{R_\pm}\right) = \frac{\rho}{R_\pm} J_1\left(\frac{\rho j_{1n}}{R_\pm}\right) \exp(\pm i k_n^\pm z) \tag{22}$$

where $n=1,2,3,\cdots$

$$\int_0^1 \frac{dx}{x} F_n(x) F_m(x) = \frac{1}{2} J_0(j_{1n})^2 \delta_{nm} \tag{23}$$

$$\left(k_n^\pm\right)^2 = \frac{\omega^2}{c^2} - \frac{j_{1n}^2}{R_\pm^2} \tag{24}$$

$$J_1(j_{1n}) = 0 \tag{25}$$

Suppose that $\left(k_n^\pm\right)^2$ is positive for $n=0,1,2,\cdots N^\pm$, and negative otherwise. Then all modes with $n > N_\pm$ will decay as one advances out of the taper towards the $\begin{pmatrix}\text{right}\\ \text{left}\end{pmatrix}$ dying out in a distance of the order of $\left|k^\pm_{(N_\pm+1)}\right|^{-1}$. Thus far to the left of the taper, Ψ can be well represented by the finite series

$$\Psi(\rho,z) = \sum_{n=0}^{N_-} \alpha_n^- F_n\left(\frac{\rho}{R_-}\right) \exp\left(ik_n^- z\right) + \sum_{n=0}^{N_-} \beta_n^- F_n\left(\frac{\rho}{R_-}\right) \exp\left(-ik_n^- z\right) \tag{26}$$

Assume that the source of the radiation is on the left. This corresponds to stipulating on the segment Γ_- of the boundary curve Γ, that is at a point z_- sufficiently far to the left of the taper so that the evanescent modes generated by the taper have died out, the coefficients

α_n^- of the rightward propagating modes. Moreover one must require on the segment Γ_+ of the boundary Γ, that is at a point z_+ sufficiently far to the right that all the evanescent modes generated by the taper have died out, that the coefficients β_n^+ of the leftward propagating solution vanish, corresponding to the absence of a source on the right, namely that

$$\Psi(\rho,z) = \sum_{n=0}^{N_+} \alpha_n^+ F_n\left(\frac{\rho}{R_+}\right) \exp\left[ik_n^+(z-z_+)\right] \tag{27}$$

Also Ψ must vanish on the segment Γ_w corresponding to the perfectly conducting wall. The task is thus to find the coefficients α_n^+ and β_n^-. On the perfectly conducting wall, the segment Γ_w, one must require that Ψ=0. As we shall see in section 4, this is accomplished by decomposing the problem into a number of simpler problems such that the answer is the sum of the solutions of these simpler cases.

The case of a microwave horn is shown schematically in Figure 2. The mathematical problem is the same as that of the tapered waveguide except that the curve Γ_+ has moved off to infinity where Ψ must vanish, which feature is automatic because of the asymptotic properties of the Green's function. On the outside of the horn the segment of Γ there is terminated sufficiently far to the left that the diffracted field is negligible. As in the case of the tapered waveguide one has to stipulate the α_n^- and determine the β_n^-. On the perfectly conducting wall, the segment Γ_w, one must require that Ψ=0.

For the case of a scatterer as shown schematically in Figure 3, the domain of interest is that external to the object. One must give the incident wave Ψ_{in}, for example a plane wave e^{ikz}. It is then convenient to write $\Psi = \Psi_{in} + \Psi_s$. On the scatterer, the segment Γ_w, where the electric field and hence Ψ must vanish, the scattered wave Ψ_s satisfies $\Psi_s(\rho(s),z(s)) = -\Psi in$, where s denotes arc length along the curve Γ, the intersection of the outside of the scatterer and a plane of constant azimuth ϕ. Clearly one can deal with the case where the scatterer is inside a waveguide or horn in a parallel way by combining the problems already described.

For a closed cavity the domain is the interior of the object, the hatched region of Figure 2. In this case the frequency ω is not determined by an external agency, rather it is found to be an eigenvalue, of which there are an infinite denumerable set. It is is readily seen that the eigenvalues ω^2 are all real and positive. One multiplies (5) by Ψ^* and integrates over the

volume of the cavity, whence on using Gauss's theorem and the requirement that Ψ vanish on the metallic wall it follows, even when ε and μ are functions of position, that

$$\omega^2 = \frac{\int d^3r \frac{|\nabla\Psi|^2}{\mu\rho^2}}{\int d^3r \frac{\varepsilon|\Psi|^2}{\rho^2}} \geq 0 \qquad (28)$$

For the cavity the term $\phi(s')$ in (15) vanishes, the integral equation is homogeneous, and has solutions only for characteristic values of ω^2.

For the case of an open cavity, like the open resonator shown schematically in Figure 4, the associated integral equation is homogeneous, but the eigenvalues are complex because of radiation loss. The most interesting case of low loss systems where the eigenvalues are almost real, can be dealt with very efficiently and the least lossy eigenvalues found efficiently.

4. Reduction of Problems I and II to Sequences of Dirichlet Problems

While the problems presented in section 3 are well-posed, the analytical and numerical apparatus for dealing with them is not as well developed as that for classical problems of mathematical physics, such as Dirichlet and Neumann problems for the Helmholtz equation[3]. Therefore, we will reduce them to finite sequences of Dirichlet problems for (5) on perspicuously constructed regions, and later deal with them numerically .

Consider the case of the horn depicted in Figure 2. Recall that one stipulates the waves incident from the left on Γ_- (at $z=z_-$) by giving the coefficients α_n^- in (26), and requires that Ψ vanish on the metallic wall corresponding to the curve Γ_w. In order to deal with this situation and determine the unknown coefficients β_n^- characterizing the reflected waves we construct a finite sequence of auxiliary functions Φ_i defined in the domain Ω in ρ,z interior to the curve $\Gamma=\Gamma_-+\Gamma_w$ + the sector of a circle the radius of which tends to infinity, as indicated in Figure 2. The desired solution Ψ can be expressed as a linear combination of these and the coefficients determined in a convenient manner.The ϕ_j are solutions of the following Dirichlet problem (where for the horn problem we suppress any unnecessary superscripts and subscripts $-$).

a) For all $m = 1,2,\ldots,2N$, Φ_m satisfies Equation (32) inside Ω.
b) For all $m = 1,2,\ldots,2N$, Φ_m vanishes on Γ_w. (29)
c) For all $m = 1,2,\ldots,N$, on Γ_-

$$\Phi_m = F_m\left(\frac{\rho}{R}\right)\exp(ik_m z) \tag{30}$$

d) For all m = n+1,n+2,...,2n, on Γ_-

$$\Phi_m = F_m\left(\frac{\rho}{R}\right)\exp\left(ik_{N-m}z\right) \tag{31}$$

Far to the left of the end of the horn each of the ϕ_m must have a representation of the form of (26), namely

$$\Phi_m(\rho,z) = \sum_{n=1}^{N} A_{m,n} F_n\left(\frac{\rho}{R}\right)\exp(ik_n z) + \sum_{n=1}^{N_-} B_{m,n} F_n\left(\frac{\rho}{R}\right)\exp(-ik_n z) \tag{32}$$

Write

$$\Psi(\rho,z) = \sum_{m=1}^{2n} \gamma_m \Phi_m(\rho,z) \tag{33}$$

Then on using both (26) and (32) combined with (33) to express Ψ there results

$$\sum_{m=1}^{2n}\gamma_m \sum_{n=1}^{N} A_{m,n}F_n\left(\frac{\rho}{R}\right)\exp(ik_n z) + \sum_{m=1}^{2n}\gamma_m \sum_{n=1}^{N} B_{m,n}F_n\left(\frac{\rho}{R}\right)\exp(-ik_n z)$$
$$= \sum_{n=0}^{N}\alpha_n F_n\left(\frac{\rho}{R}\right)\exp(ik_n z) + \sum_{n=0}^{N}\beta_n F_n\left(\frac{\rho}{R}\right)\exp(-ik_n z) \tag{34}$$

Multiply (34) by $F_s\left(\frac{\rho}{R_-}\right)$. Then in virtue of the orthogonality condition (23) it follows on replacing s by n that for n=1,2,3...N

$$\sum_{m=1}^{2N_-} \gamma_m A_{m,n} \exp(ik_n) + \sum_{m=1}^{2N_-} \gamma_m B_{m,n} \exp(-ik_n z) = \alpha_n \exp(ik_n z) + \beta_n \exp(-ik_n z) \tag{35}$$

The coefficients of $\exp(ik_n z)$ and $\exp(-ik_n z)$ in (35) must vanish separately, as can be seen by multiplying (35) by $\exp(\pm ik_n z)$ and integrating with respect to z over a distance $2\pi/k_n$. Thus for n=1,2,3...N_

$$\sum_{m=1}^{2N_-} \gamma_m A_{m,n} = \alpha_n$$
$$\sum_{m=1}^{2N_-} \gamma_m B_{m,n} = \beta_n \tag{36}$$

Eqs. (36) are a system of $2N_-$ linear equations for the unknown N_- coefficients γ_m and the unknown N_- coefficients β_m. With the coefficients thus determined (33) is the desired solution since it satisfies the differential equation (6) and all the boundary conditions.
For the case of the tapered waveguide the procedure is similar. The domain Ω is defined by the z axis and the curve $\Gamma=\Gamma_- \cup \Gamma_w \cup \Gamma_+$ (see Figure 1). One defines auxiliary functions Φ_m as follows.

a) For all m = 1,2,...,$2N_-$, Φ_m satisfies Equation (32) inside Ω.
b) For all m = 1,2,...,$2N_-$, Φ_m vanishes on $\Gamma_w + \Gamma_+$. (37)
c) For all m = 1,2,...,N_-, on Γ_-

$$\Phi_m = F_m\left(\frac{\rho}{R_-}\right)\exp\left(ik_m^- z\right) \tag{38}$$

d) For all m = $N_-+1, N_-+2, \ldots, 2N_-$, on Γ_-

$$\Phi_m = F_m\left(\frac{\rho}{R_-}\right)\exp\left(-ik_{m-N_-}^+ z\right) \tag{39}$$

One defines auxiliary functions functions Ψ_m such that

a) For all $m = 1,2,\ldots,2N_+$, Ψ_m satisfies Equation (32) inside Ω.
b) For all $m = 1,2,\ldots,2N_+$, Ψ_m vanishes on $\Gamma_w + \Gamma_-$.
c) For all $m = 1,2,\ldots,N_+$, on Γ_+ (40)

$$\Psi_m = F_m\left(\frac{\rho}{R_+}\right)\exp\left(ik_m^+ z\right) \tag{41}$$

d) For all $m = N_+{+}1, N_+{+}2, \ldots, 2N_+$, on Γ_+

$$\Psi_m = F_m\left(\frac{\rho}{R_+}\right)\exp\left(-ik_{m-N_+}^+ z\right) \tag{42}$$

Then far to the right of the taper

$$\Phi_m(\rho,z) = \sum_{n=1}^{N_+} A_{m,n}^{-,+} F_n\left(\frac{\rho}{R_+}\right)\exp\left(ik_n^+ z\right) + \sum_{n=1}^{N_+} B_{m,n}^{-,+} F_n\left(\frac{\rho}{R_+}\right)\exp\left(-ik_n^+ z\right) \tag{43}$$

$$\Psi_m(\rho,z) = \sum_{n=1}^{N_+} A_{m,n}^{+,+} F_n\left(\frac{\rho}{R_+}\right)\exp\left(ik_n^+ z\right) + \sum_{n=1}^{N_+} B_{m,n}^{+,+} F_n\left(\frac{\rho}{R_+}\right)\exp\left(-ik_n^+ z\right) \tag{44}$$

and far to the left of the taper

$$\Phi_m(\rho,z) = \sum_{n-1}^{N_-} A_{m,n}^{-,-} F_n\left(\frac{\rho}{R_-}\right)\exp\left(ik_n^- z\right) - \sum_{n-1}^{N_-} B_{m,n}^{-,-} F_n\left(\frac{\rho}{R_-}\right)\exp\left(-ik_n^- z\right) \tag{45}$$

$$\Psi_m(\rho,z) = \sum_{n-1}^{N_-} A_{m,n}^{+-} F_n\left(\frac{\rho}{R_-}\right)\exp\left(ik_n^- z\right) - \sum_{n-1}^{N_-} B_{m,n}^{+-} F_n\left(\frac{\rho}{R_-}\right)\exp\left(-ik_n^- z\right) \quad (46)$$

The coefficients in (43) - (46) are determined by evaluating the solutions of the integral equations for Φ_n and Ψ_n at an appropriate number of suitably chosen points.

Next one writes

$$\Psi(\rho,z) = \sum_{m=1}^{2N_-}\gamma_m\Phi_m + \sum_{m=1}^{2N_+}\eta_m\Psi_m \quad (47)$$

On equating the asymptotic representations (26) and (27) on their respective domains of validity , and using the orthogonality of the F_n and integration over z as was done for the horn , one obtains the algebraic system

$$\sum_{m=1}^{2N_-} A_{m,n}^{-+}\gamma_m + \sum_{m=1}^{2N_+} A_{m,n}^{++}\eta_m = \alpha_n^+ \quad (48)$$

$$\sum_{m=1}^{2N_-} A_{m,n}^{--}\gamma_m + \sum_{m=1}^{2N_+} A_{m,n}^{+-}\eta_m = \alpha_n^-(\text{given}) \quad (49)$$

$$\sum_{m=1}^{2N_-} B_{m,n}^{-+}\gamma_m + \sum_{m=1}^{2N_+} B_{m,n}^{++}\eta_m = \beta_n^+ = 0 \quad (50)$$

$$\sum_{m=1}^{2N_-} B_{m,n}^{--}\gamma_m + \sum_{m=1}^{2N_+} B_{m,n}^{+-}\eta_m = \beta_n^- \quad (51)$$

Eqs. (48) - (51) are a set of $2(N_- + N_+)$ linear equations for the N_- complex numbers γ_m, the N_+ complex numbers η_m, the N_- complex numbers β_n^-, and the N_+ complex numbers α_n^+. Once these have been found the solution $\Psi(\rho,z)$ is completely known via (47), and transmission and reflection are determined by the coefficients α_n^+ and β_n^-.

5-Nystrom method for the solution of second kind integral equations (SKIEs)

We have reduced the problem of determining the electric field to consideration of (15), a second kind integral equation (SKIE). This can be dealt with numerically by discretization via an appropriate quadrature formulae.

We will define an n-point quadrature rule on the interval [0,L] as a finite sequence of pairs $\{x_1, w_1\}$, i=1,2,....n, where $x_1 \in [0,L]$ for all $i \in [1,n]$. For a function ψ : $[0,L] \rightarrow R^1$, we will look upon the sum

$$\eta(\psi) = \sum_{i=1}^{n} w_i \psi(x_i) \tag{52}$$

as an approximation to the integral

$$\int_0^L \psi(x)dx \ . \tag{53}$$

For the cases considered, we treat L is the length of the arc Γ. We will say that the family of quadrature formulae $\left\{\eta_n = \left\{x_n^i, w_n^i\right\}, i = 1,2,\ldots,n\right\}$, n = 1,2,..., has a convergence rate m ($m \geq 1$) for the function $\psi : [0,L] \rightarrow R^1$, if there exist numbers A>0 and integers N>0 such that

$$\left| \eta_n(\psi) - \int_0^L \psi(x)dx \right| < \frac{A}{n^m} \tag{54}$$

for all $n > N$.

In order to solve the integral equation

$$\sigma(x) + \int_0^L F(t,x)\ \sigma(t)\ dt \ = \ \phi(x) \tag{55}$$

the Nystrom algorithm replaces (32) with a system of linear algebraic equations

$$\sigma_i + \sum_{j=1}^{n} w_i^j \, F(x_j,x_i) \, \sigma_j = \phi(x_i), \tag{56}$$

with $i = 1,2,\ldots,n$, and $w_i^1, w_i^2, \ldots, w_i^n$ the coefficients of an appropriately chosen quadrature formulae. We will denote the matrix of the system (27) by A_n, and view the solution $\sigma_1,\sigma_2,\ldots,\sigma_n$ of (27) as an approximation to the solution Ψ of (26) at the nodes $x_1,x_2,\ldots, x_n$.

Note that in general, the coefficients $w_i^1, w_i^2,\ldots,w_i^n$ of the quadrature formula depend on the point x_i at which the integral (32) is being approximated. When the kernel F is smooth, this can be avoided by choosing a single quadrature formula, such as the end-point corrected trapezoidal rule, that will perform well for all $i = 1,2,\ldots,n$. However, in many applications the kernel is singular, and the distribution of its singularities usually forces a special choice of a quadrature formula for each node.

The following theorem [4] is the principal justification for the use of the Nystrom algorithm for the solution of SKIEs . Suppose that Equation (32) has a unique solution, and that its kernel F and right-hand side ϕ are continuous. Suppose further that a family $\{\eta_n^i\}$ of quadrature formulae is such that for some $B > 0$

$$\sum_{i=1}^{n} | w_i^n | \leq B \tag{57}$$

for all $n = 1,2,\ldots$. Then there exists a number $C > 0$ such that for any $n \geq 2$ and $i = 1,2,\ldots,n$,

$$| \phi_i - \tilde{\Psi}(x_i) | \leq \frac{C}{n^k} \tag{58}$$

where k is the convergence rate of the formulae $\{\eta_n^i\}$.

5. Description of the Algorithms

Now, armed with the apparatus developed in the preceding sections, we are prepared to construct algorithms for the solution of the original problems in Section 3. First, we describe an algorithm for the solution of the horn problem.

Algorithm I

Step 1. Construct the curve Γ by appending the segment Γ_- to the user-specified waveguide boundary (see Figure 5). Use spline package FITPACK[5] to construct an equi-spaced discretization of the resulting curve. Select the N nodes into which the boundary Γ is to be discretized.

Step 2. Convert the problem into a sequence of exterior Dirichlet problems in the region Ω as described in section 4. For each i = 1,2,...,2N, convert the corresponding Dirichlet problem into a second kind integral equation (SKIE) on Γ.

Step 4. For each i = 1,2,...,2N, discretize the obtained SKIE via the Nystrom method based on the quadrature formulae of Appendix C, obtaining a system of linear algebraic equations of dimension 2N .

Step 5. For each i = 1,2,...,2N, solve the linear system obtained on the preceding step by means of a standard Gaussian elimination subroutine from LINPACK [6]. View the solution as an approximation to σ on Γ solving the underlying Dirichlet problem.

Step 6. Find the coefficients $\gamma_1,\gamma_2,\ldots,\gamma_{2N}$ in equation (33) by solving (36)

Step 7. Linearly combine the solutions of the 2N linear systems obtained on the preceding step according to the formula (33). The result is a distribution σ on γ_2 whose field is a solution of the problem .

Step 8. For each point $x \in R^2$ where the solution of the horn problem is desired, evaluate it by approximating the integral

$$\int_{\Gamma} \sigma(t)\, G(x,t)\, dt \qquad (59)$$

by the trapezoidal sum

$$h \sum_{i=1}^{N} \sigma(t_i)\, G(t_i,x) \qquad (60)$$

with $\{t_i\}$, i = 1,2, $\cdots$ N, the nodes in the discretization of Γ, and h the sampling distance between the adjacent nodes t_i, t_{i-1}.

Next we describe an algorithm for the solution of the tapered waveguide problem .

Algorithm 2

Step 1. Construct the curve Γ by appending the segments Γ_+, and Γ_- to the desired part of the boundary of the user-specified waveguide Γ (see Figure 1). Use spline package FITPACK [5] to construct an equispaced discretization of the resulting curve. Select the number N of nodes into which the boundary Γ is to be discretized.

Step 2. Convert the problem into a pair of sequences of interior Dirichlet problems in the region Ω.

Step 3. For each $i = 1,2,\ldots,2N_-$, convert the corresponding Dirichlet Problem into a second kind integral equation on Γ.

Step 4. For each $i = 1,2,\ldots,2N_+$, convert the corresponding Dirichlet Problem into a second kind integral equation on Γ.

Step 5. For each $i = 1,2,\ldots,2\cdot N_-$, discretize the obtained SKIE via the Nystrom method based on the quadrature formulae of Appendix C, obtaining a system of linear algebraic equations of dimension N

Step 6. For each $i = 1,2,\ldots,2N_-$, discretize the obtained SKIE via the Nystrom method based on the quadrature formulae of Appendix C, obtaining a system of linear algebraic equations of dimension N.

Step 7. For each $i = 1,2,\ldots,2N_-$, solve the linear system obtained on the preceding step by means of a standard Gaussian elimination subroutine from LINPACK [6]. View the solution as an approximation to the density σ on Γ solving the underlying Dirichlet Problem

.

Step 8. For each $i = 1,2,\ldots,2N_+$, solve the linear system obtained on the preceding step by means of a standard Gaussian elimination subroutine from LINPACK. View the solution as an approximation to the density of dipole distribution on Γ solving the underlying Dirichlet problem.

Step 9. Find the coefficients $\gamma_1,\gamma_2,\ldots,\gamma_{2N_-}$ and $\eta_1,\eta_2,\ldots,\eta_{2N_-}$ in the expansion (47)

Step 10. Linearly combine the solutions of the $2(N_- + N_+)$ linear system obtained on the preceding step according to the formula (47). The result is a distribution σ on Γ whose field is a solution of the tapered waveguide problem.

Step 11. For each point $x\in\Omega$ where the solution of problem is desired, evaluate it by approximating the integral

$$\int_{\Gamma} \sigma(t)\, F(x,t)\, dt \tag{61}$$

by the trapezoidal sum

$$h \sum_{i=1}^{N} \sigma(t_i)\ F(t_i,x) \tag{62}$$

with $\{t_i\}$, $i = 1,2,\ldots,N$ the nodes in the discretization of G3, and h the sampling distance between the adjacent nodes t_i, t_{i-1}.

6-Results

A fortran program has been written implementing algorithms I and II of this paper. The program has been tested on a variety of problems. We present a detailed description and the results of four such numerical experiments.

Example 1 - Tapered Waveguide

The waveguide defined in fig. 5 has a left hand asymptotic radius of 0.524 cm. and a right hand asymptotic radius of 0.743 cm . The shape was assigned by stipulating a dense set of points, which were then fitted to a spline, a convenient design procedure. The transition distance is roughly 2.5 cm. The operating frequency chosen is $3.2X10^{11}$ sec^{-1}. This leads to one propagating mode on the far left of the tapered section , and two propagating modes on the far right. The boundary employed for the calculation was first approximated as shown in fig. 6, adding the piecewise linear curves Γ_+ and Γ_- to provide a closed bounding surface for the three dimensional domain obtained by rotating the boundary around the z axis. This shape was then resampled to provide the smooth curve of fig.7, which was then discretized into 90 roughly equally spaced nodes. Also indicated are the test points employed in computing the modal expansion of the solution. The results for the lines of constant real part of Ψ are displayed in fig. 8. The calculation took six minutes of CPU time on a VAX 780.

Example 2 - Open Waveguide

This calculation uses a semi-infinite waveguide of 2 cm. inner radius and 0.25 cm. thickness. The operating frequency is $6x10^{10}$ sec^{-1}, resulting in one propagating mode on the far left. The resampled boundary is shown in fig. 9. This was discretized into 180 nodes, with the points most dense in the neighborhood of the return in the boundary curve at the end of the waveguide . The calculation took 17 minutes of CPU time on a Vax 8600. The resulting lines of constant real part of Ψ are shown in fig. 10. The resulting radiation pattern is shown in fig. (11) where $|f(\theta)|^2 = |E|^2/r^2$ is plotted vs. the polar angle θ that the direction of observation makes with the axis if the waveguide.

Example 3 - Microwave Horn

The internal far left radius of the horn is 2 cm., and its wall thickness 0.25 cm. The frequency employed is $6x10^{10}$ sec^{-1}, yielding one propagating mode on the far left. The resampled boundary is shown in fig. 12. It was discretized into 180 nodes, with the nodal density greatest near the return in the curve. The calculation took 17 minutes of CPU time on a Vax 8600. The lines of constant imaginary part of Ψ are shown in fig. 13. The radiation pattern is displayed in fig. 14, where $|f(\theta)|^2 = |E|^2/r^2$ is plotted vs. the polar angle θ that the direction of obervation makes with the axis if the waveguide.

Example 4 - Injection Trough a Hole in a Metallic Wall

The far left radius of the waveguide is 3 cm. and its wall thickness is 2 cm. The frequency employed is $6x10^{10}$ sec^{-1}, yielding one propagating mode on the far left. The resampled boundary is shown in fig. 17. It was discretized into 180 nodes. The calculation took 13 minutes on a Vax 8600. The lines of constant real part of Ψ are shown in fig. 17 and the lines of constant imaginary part of Ψ are displayed in fig. 17. The radiation pattern is displayed in fig. 18, where $|f(\theta)|^2 = |E|^2/r^2$ is plotted vs. the polar angle θ that the direction of observation makes with the axis if the waveguide.

Appendix A - The Green's Function

Recall that $R = |r - r'| = \left[\rho^2+\rho'^2-2\rho\rho'\cos(\phi-\phi')+(z-z')^2\right]^{1/2}$ where ρ,ϕ,z are cylindrical coordinates. Then the three dimensional Green's function

$$G = \frac{e^{ikR}}{4\pi R} \tag{A1}$$

satisfies

$$\nabla^2 G + k^2 G = -\delta(r - r') = -\frac{\delta(\rho - \rho')\delta(z - z')\delta(\phi - \phi')}{\rho'} \tag{A2}$$

Write

$$G(\rho,\rho',\phi-\phi',z-z') = F(\rho,\rho',\phi-\phi',z-z')\, e^{i(\phi-\phi')} \tag{A3}$$

Then it is readily calculated on using the properties of the Dirac delta function that

$$\nabla^2 F + \frac{2i}{\rho}\frac{\partial f}{\partial \phi} + \left(k^2 - \frac{1}{\rho^2}\right)F = -\frac{\delta(\rho - \rho')\delta(z - z')\delta(\phi - \phi')}{\rho'} \tag{A4}$$

Let

$$\bar{F}(\rho,\rho',z-z') = \int_0^{2\pi} d\phi\, F(\rho,\rho',\phi-\phi',z-z') \tag{A5}$$

Then it follows from (A4) on integrating over one period in ϕ that

$$\nabla^2 \bar{F} + \left(k^2 - \frac{1}{\rho^2}\right)\bar{F} = -\frac{\delta(\rho-\rho')\delta(z-z')}{\rho'} \tag{A6}$$

Define

$$K(\rho,\rho',z-z') = \rho\rho'\,\bar{F}(\rho,\rho',z-z') = \rho\rho' \int_0^{2\pi} d\phi\, e^{-i(\phi-\phi')} G(\rho,\rho',\phi-\phi',z-z') \tag{A7}$$

Note that K is invariant under interchange of primed and unprimed arguments. Then (A6) implies

$$\nabla^2\left(\frac{K}{\rho}\right) + \left(k^2 - \frac{1}{\rho^2}\right)\frac{K}{\rho} = -\delta(\rho-\rho')\delta(z-z') \tag{A8}$$

But

$$\nabla\cdot\left(\frac{\nabla K}{\rho^2}\right)=\frac{\nabla^2 K}{\rho^2}-\frac{2}{\rho^3}\frac{\partial K}{\partial \rho} \tag{A9}$$

while

$$\nabla^2\left(\frac{K}{\rho}\right)=\frac{\nabla^2 K}{\rho}-\frac{2}{\rho^2}\frac{\partial K}{\partial \rho}+\frac{K}{\rho^2} \tag{A10}$$

whence (A8) implies

$$\rho\,\nabla\cdot\left(\frac{\nabla K}{\rho^2}\right)+k^2\frac{K}{\rho}=-\delta(\rho-\rho')\delta(z-z') \tag{A11}$$

and on using the properties of the Dirac delta function

$$L\{K\}\equiv\nabla\cdot\left(\frac{\nabla K}{\rho^2}\right)+\frac{k^2}{\rho^2}K=-\frac{\delta(\rho-\rho')\delta(z-z')}{(\rho\rho')^{1/2}} \tag{A12}$$

We wish to derive an integral representation for Ψ of the form

$$\Psi'\equiv\Psi(\rho',z')=\int_{\Gamma} ds\;\sigma(s)\left[\mathbf{n}\cdot\nabla K(\rho,\rho',z-z')\right]_{\rho=\rho(s)\;\;z=z(s)} \tag{A13}$$

where Γ is that curve which when rotated around the z axis generates the surface S enclosing the volume V containing the point r'. The element of arc length along C is ds. Note that in virtue of its invariance under interchange of primed and unprimed arguments it follows from (A11) that K satisfies $L'\{K\}=0$, whence it is evident that Ψ as defined by (A16) satisfies $L'\{\Psi'\}$ at all points ρ',z' interior to the domain enclosed by Γ.

In order to derive an integral equation for the function σ, assuming that Ψ is given on Γ, we consider a point on Γ corresponding to s', and a point ρ',z' inside the area in question a distance ε from Γ as measured along the unit outward pointing normal n(s') as shown in Figure 19 . Pick $\varepsilon \ll \delta \ll$ the radius of curvature at s', and break the domain of integration up into a segment of width 2δ straddling the point s', which segment may be considered locally flat, and the rest of Γ.

As ρ',z' approaches Γ one sees from (A7) that the integrand diverges. The major contributions to the integral come from the denominator in the neighborhood of $\phi=\phi'$ where $R^2=(\rho-\rho')^2+(z-z')^2+\rho\rho'(\phi-\phi')^2$. On keeping only dominant terms it follows that

$$4\pi K \approx \rho'^2 \int_{\phi'-\pi}^{\phi'+\pi} \frac{d\phi}{\sqrt{(\rho-\rho')^2+(z-z')^2+\rho'^2(\phi-\phi')^2}}$$

$$\approx 2\,\rho'^2 \int_{\phi'}^{\phi'+\pi} \frac{d\phi}{\sqrt{(\rho-\rho')^2+(z-z')^2+\rho'^2(\phi-\phi')^2}}$$

$$\approx 2\rho'\ln\left[\sqrt{(\rho-\rho')^2+(z-z')^2+\rho'^2(\phi-\phi')^2)}+\rho'(\phi-\phi')\right]_{\phi'}^{\phi'+\pi} \qquad \text{(A14)}$$

$$\approx -\,2\rho'\ln\sqrt{(\rho-\rho')^2+(z-z')^2}$$

Thus the contribution to (A15) of the segment of width 2δ can be written to good approximation as

$$I = -\sigma(s'') \int_{s'-\delta}^{s'+\delta} ds \left[n\cdot\nabla\left(\rho' \ln\sqrt{(\rho-\rho')^2+(z-z')^2}\right)\right]_{\rho=\rho(s)\ z=z(s)}$$

$$= -\sigma(s'')\rho' \int_{s'-\delta}^{s'+\delta} ds \left\{\frac{\partial}{\partial n}\ln\left[n^2+(s-s')^2\right]\right\}_{n=-\epsilon} \qquad \text{(A15)}$$

$$= 2\sigma(s'')\rho' \int_{s'}^{s'+\delta} ds \frac{\epsilon}{\epsilon^2+(s-s')^2}$$

$$= 2\sigma(s'')\rho' \arctan\frac{\delta}{\epsilon}$$

Clearly in the limit $\epsilon\to 0$ one has

$$I = 2\pi\sigma(s'')\rho' \qquad \text{(A16)}$$

Thus in the limit that the point ρ', z' lies on C eq.(15) yields

$$\frac{2\Psi(\rho(s'),z(s'))}{\rho'} = \sigma(s') + P\int_{\Gamma} ds\ \sigma(s) \left\{n\cdot\nabla\left[\frac{2K(\rho,\rho',z-z')}{\rho'}\right]\right\}_{\rho=\rho(s)\ z=z(s)} \qquad \text{(A17)}$$

where P denotes the Cauchy principle value of the integral. On introducing the definitions of (21) and (23) this is the desired integral equation.

Acknowledgement

This work was supported by the Office of Naval Research. The authors are indebted to Dr Giora Hazak for the first derivation of the Green's function.

Figure Captions

Fig. 1 Schematic diagram of a tapered waveguide.
Fig. 2 Schematic diagram of a horn.
Fig. 3 Schematic diagram of a cavity or scatterer. For the scatterer the domain is the exterior of the boundary curve, for the cavity the domain is the cross hatched interior.
Fig. 4 Schematic diagram of an open resonator.
Fig. 5 The waveguide of example 1 as specified by the user.
Fig. 6 The waveguide of example 1 after preliminary geometric processing.
Fig. 7 Resampled waveguide with test points for example 1.
Fig. 8 Equipotentials of the real part of the solution of example 1.
Fig. 9 Resampled waveguide with test points for example 2.
Fig. 10 Equipotentials of the imaginary part of the solution to example 2.
Fig. 11 Far field amplitude as a function of angle for example 2.
Fig. 12 Resampled waveguide and test points for example 3.
Fig. 13 Equipotentials for the imaginary part of the solution for example 3.
Fig. 14 Far field amplitude as a function of angle for example 3.
Fig. 15 Resampled waveguide and test points for example 4.
Fig. 16 Equipotentials for the real part of the solution for example 4.
Fig. 17 Equipotentials for the imaginary part of the solution for example 4.
Fig. 18 Field amplitude as a function of angle for example 4.

Biliography

1. I. B. Bernstein, L. K. Devringi, T. M. Smith, Int. J. Infrared and Millimeter Waves, 4 57 (1983).

2. S. W. McDonald, J. M. Finn, M. E. Read, W. M. Mannheimer, Int. J. Electronics, 61 795 (1986).

3. R. Courant, D. Hilbert, in *Methods of Mathematical Physics* (Interscience, New York 1966), pp. 164 et seq.

4. K. E. Atkinson, *A Survey of Numerical Methods for the Solution of Fredholm I Integral Equations of the Second Kind* (SIAM, Philadelphia, 1976).

5. A. K. Cline, Comm. A.C.M., 4 218 (1974).

6. J. J. Dongarra, C. B. Moler, J. R. Bunch, G. W. Stewart, *Linpack Users Guide* (SIAM, Philadelphia, 1979).

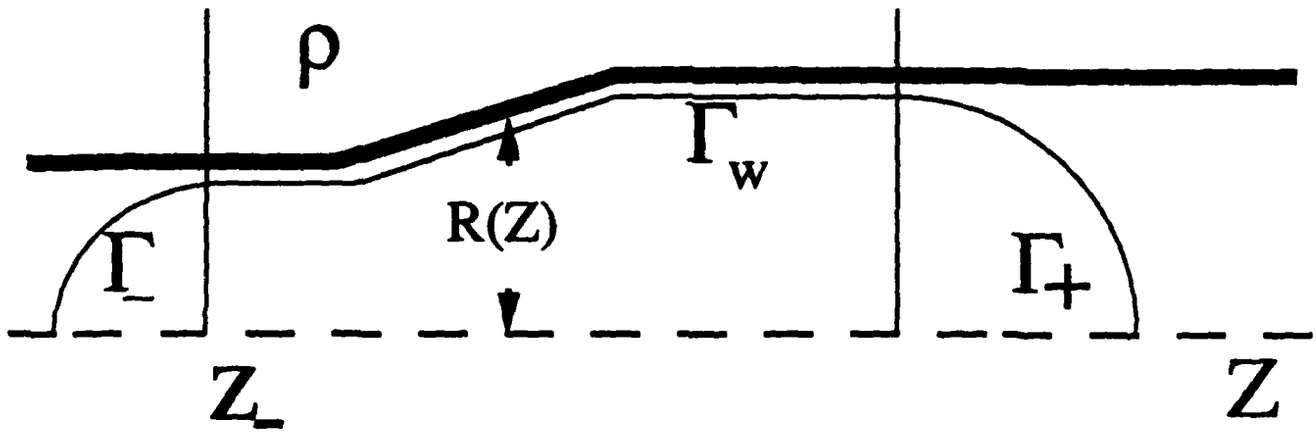

Fig. 1

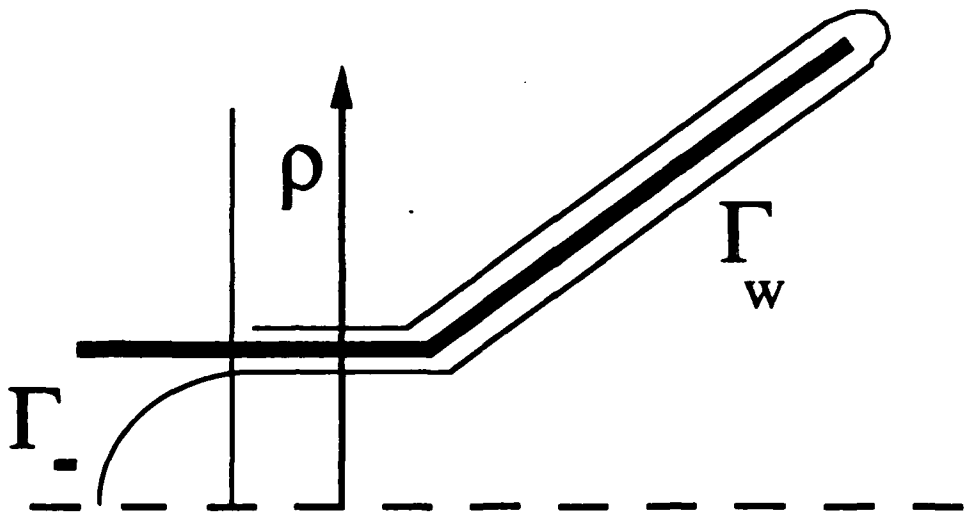

Fig. 2

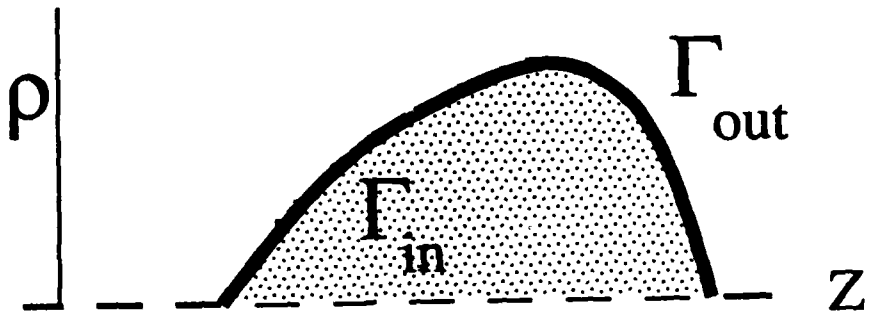

Fig. 3

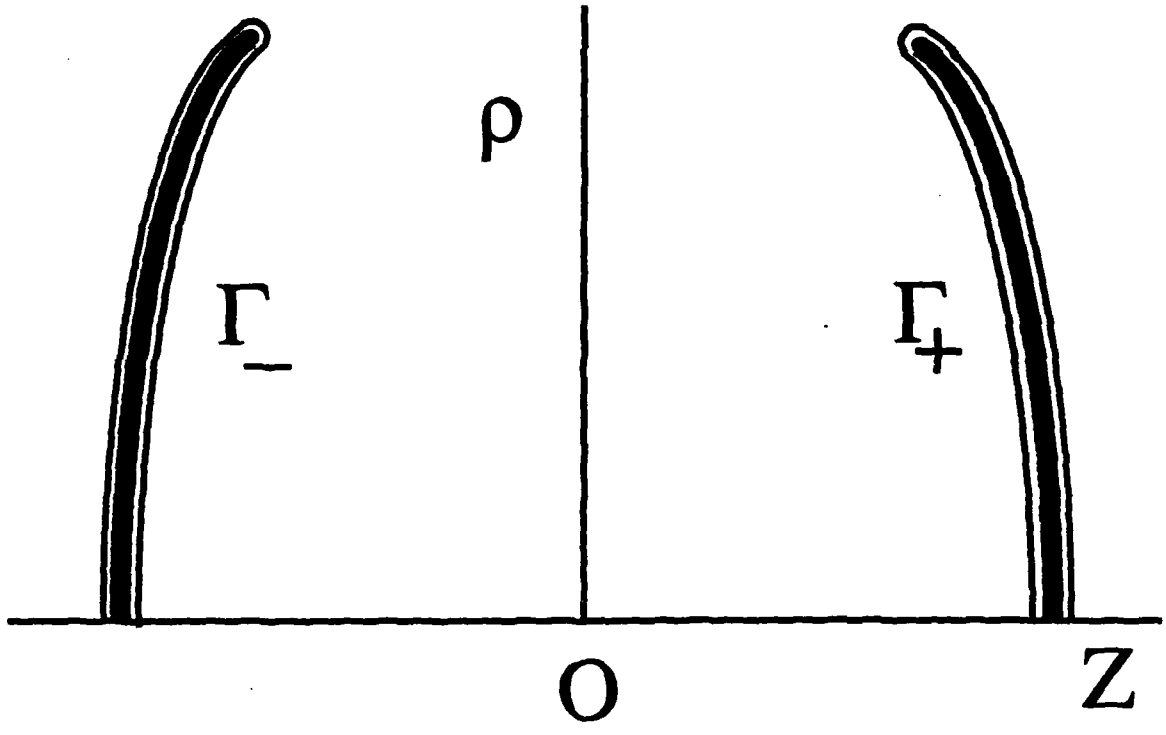

Fig. 4

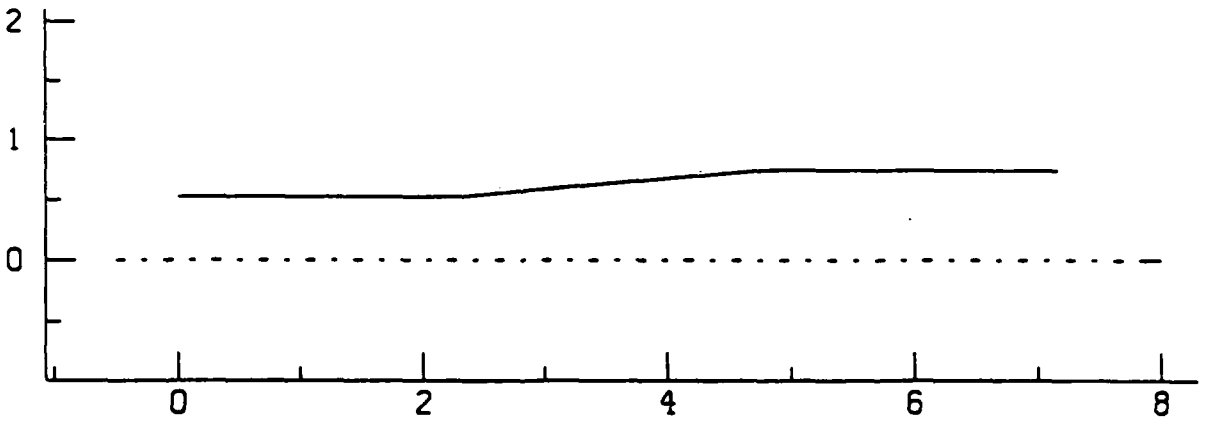

Figure 5

The Waveguide in Example 1 as Specified by the User

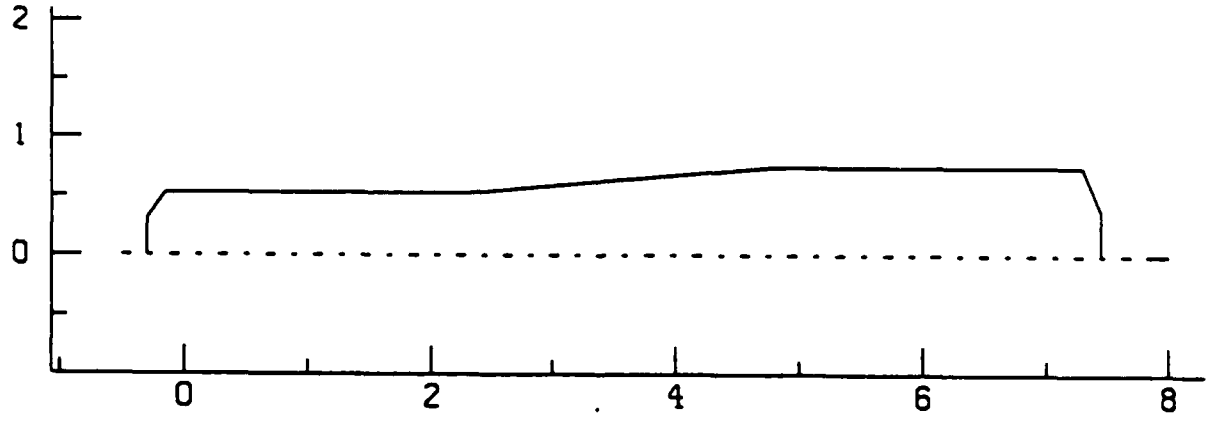

Figure 6

The Waveguide in Example 1 After Preliminary Geometrical Processing

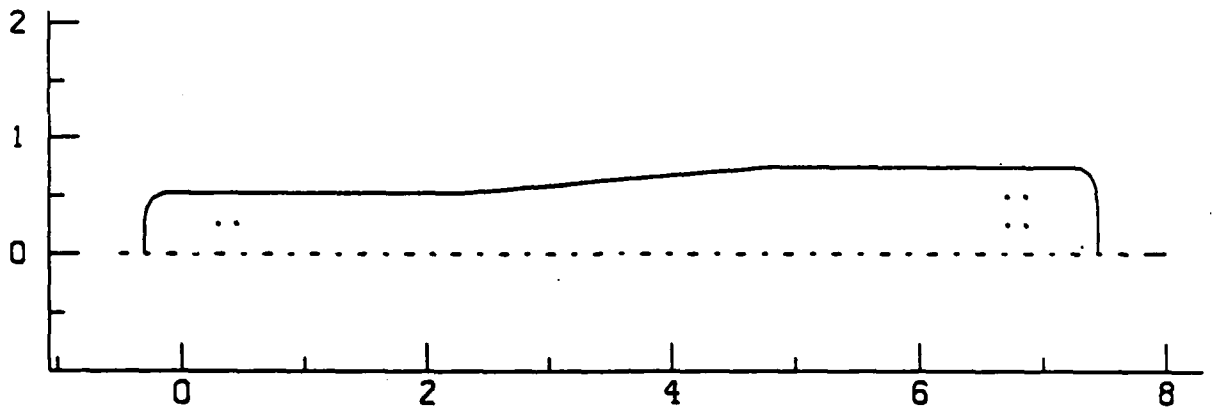

Figure 7

Resampled Waveguide with Test Points in Example 1

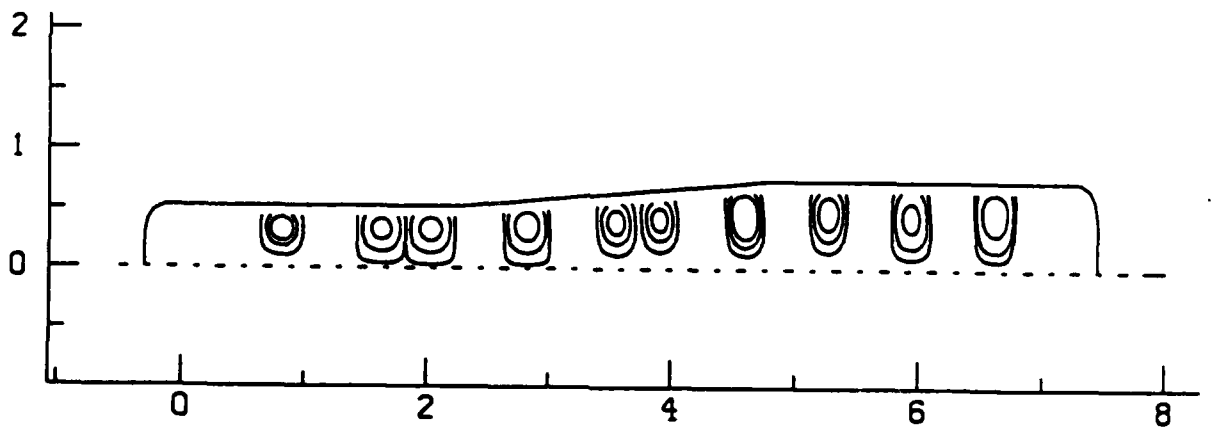

Figure 8

Equipotential Lines of the Real Part of the Solution in Example 1

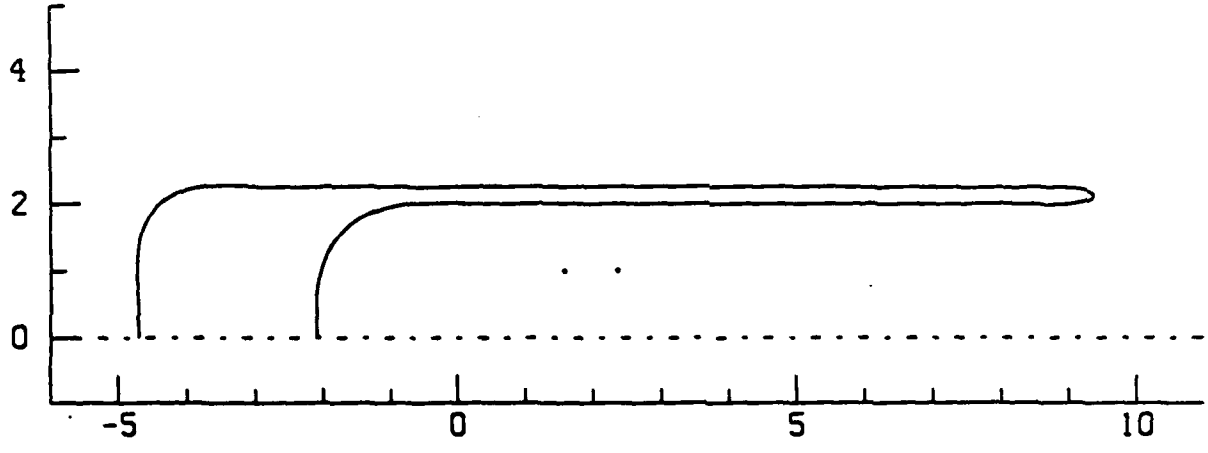

Figure 9

Resampled Waveguide with Test Points in Example 2

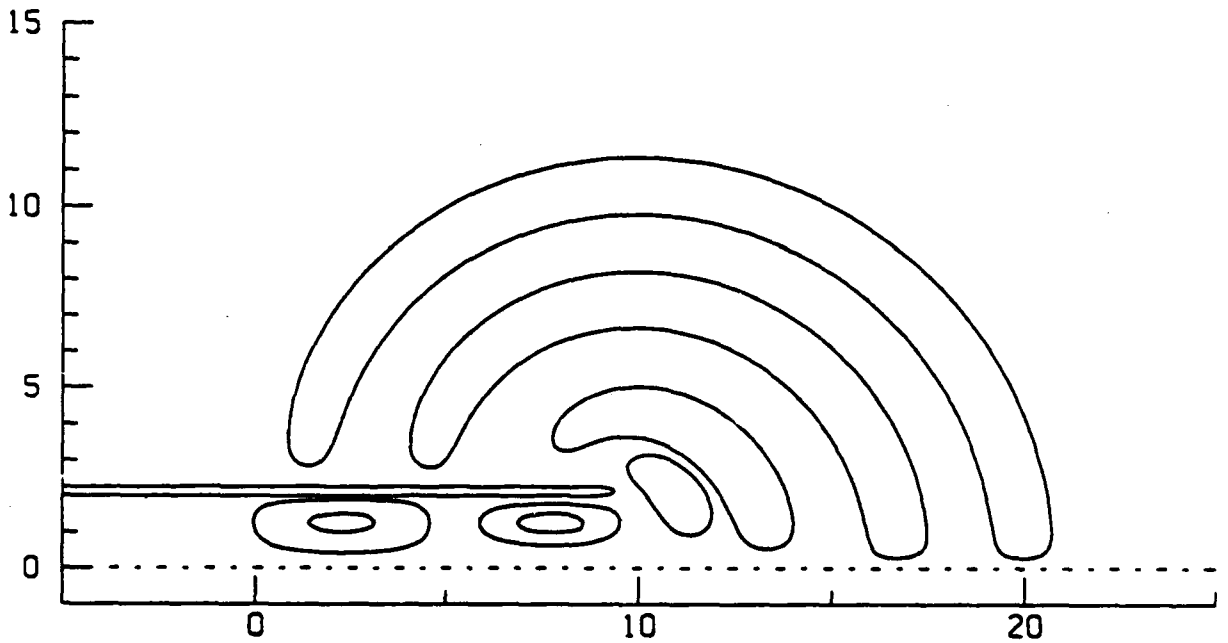

Figure 10

Equipotential Lines of the of the Imaginary Part of the Solution in the Example 2

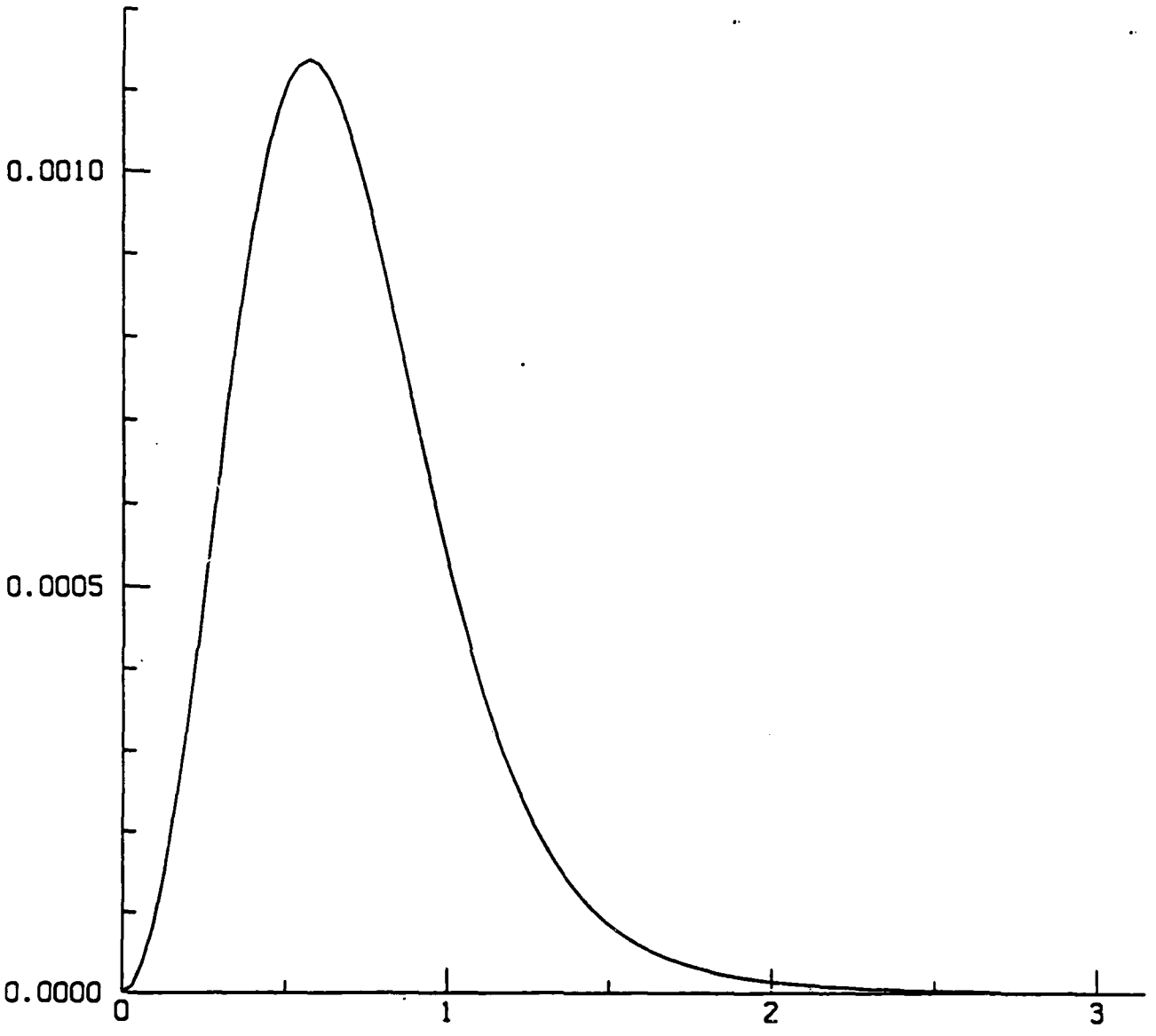

Figure 11

Far-Field Amplitude as a Function of Angle
in Example 2

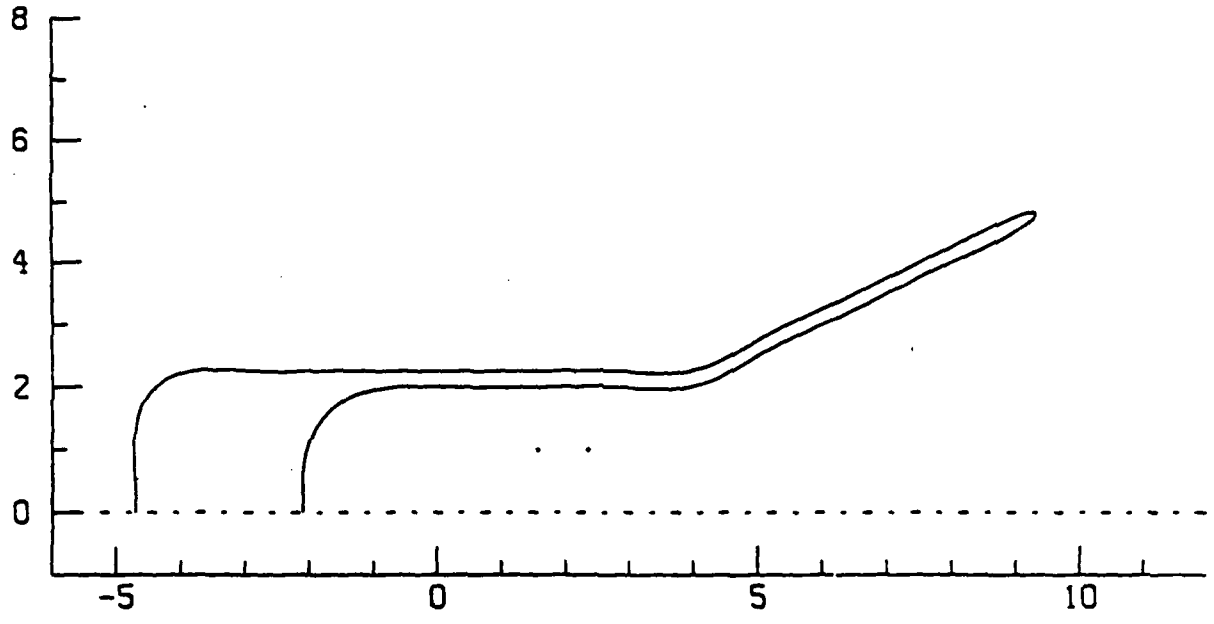

Figure 12

Resampled Waveguide with Test Points in Example 3

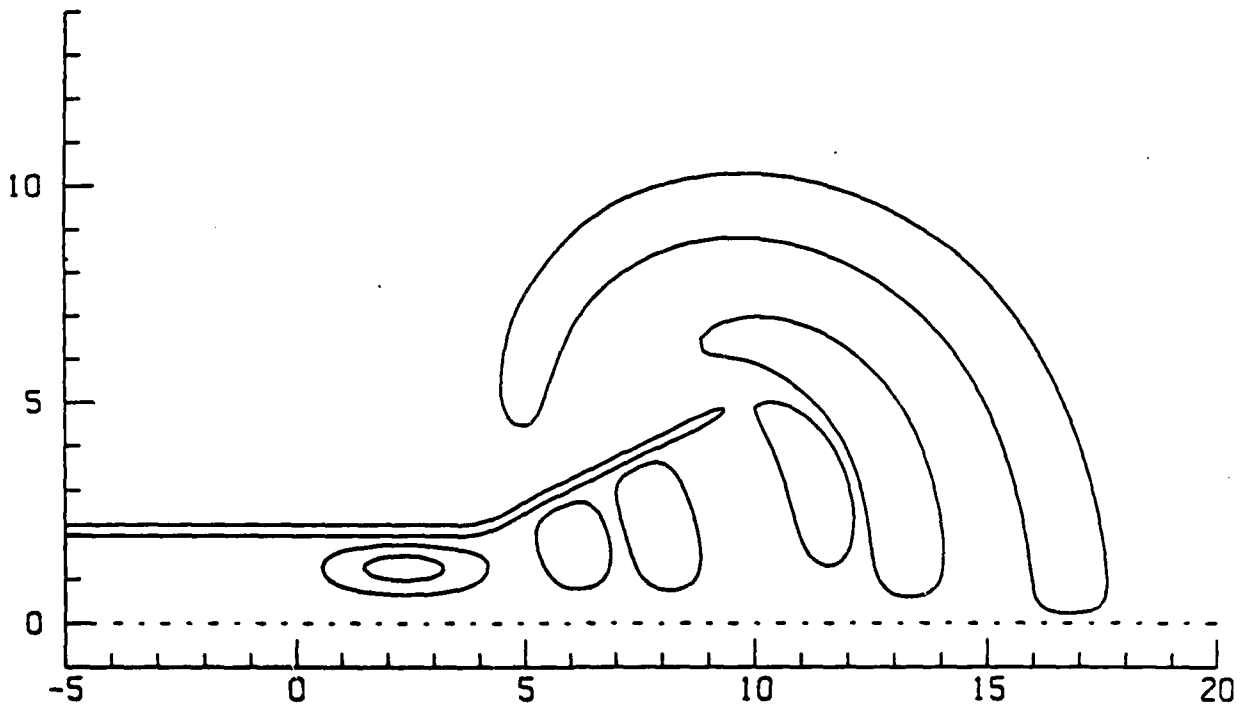

Figure 13

Equipotential Lines of the Imaginary Part of the Solution in Example 3

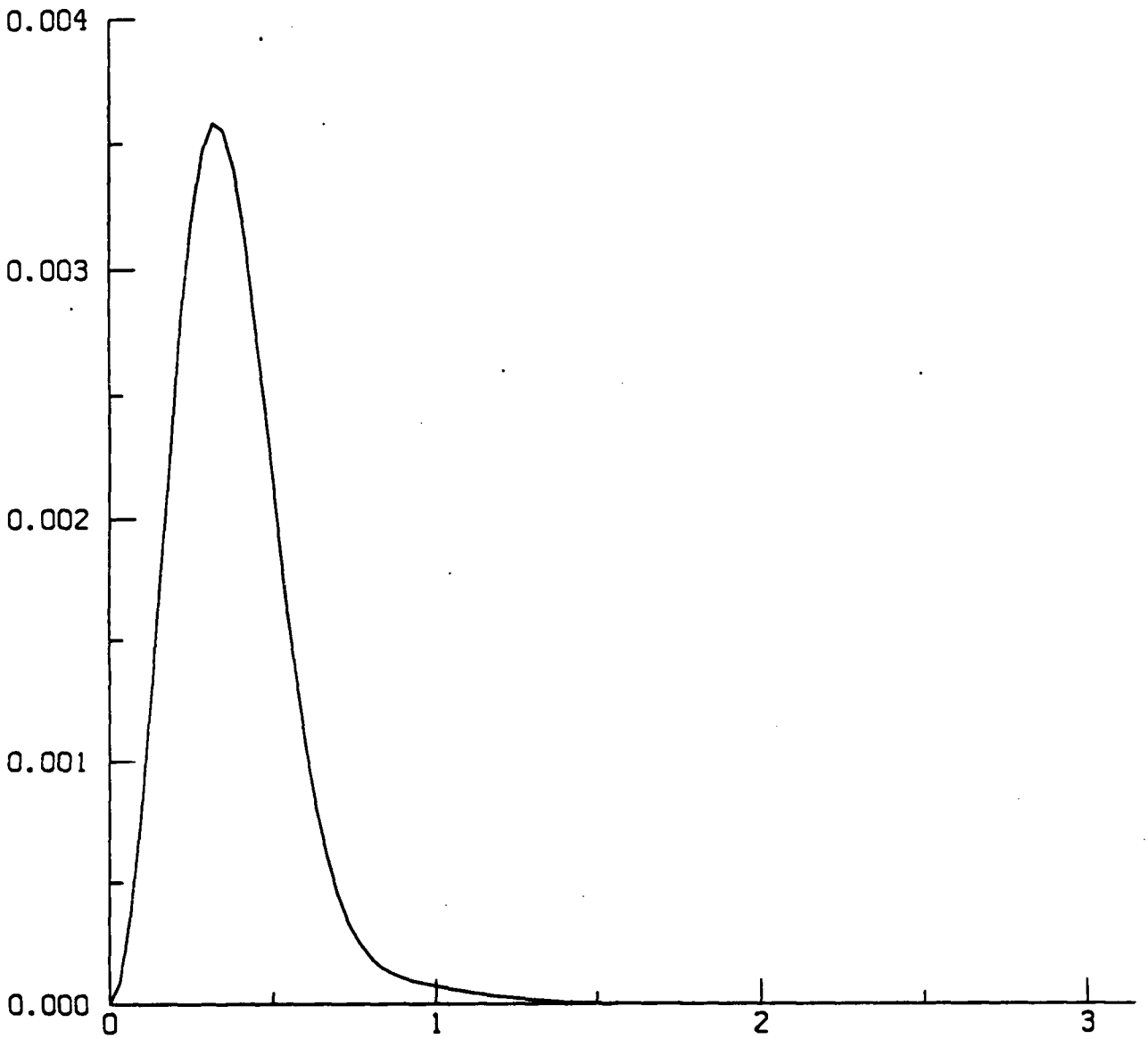

Figure 14

Far-Field Amplitude as a Function of Angle
in Example 3

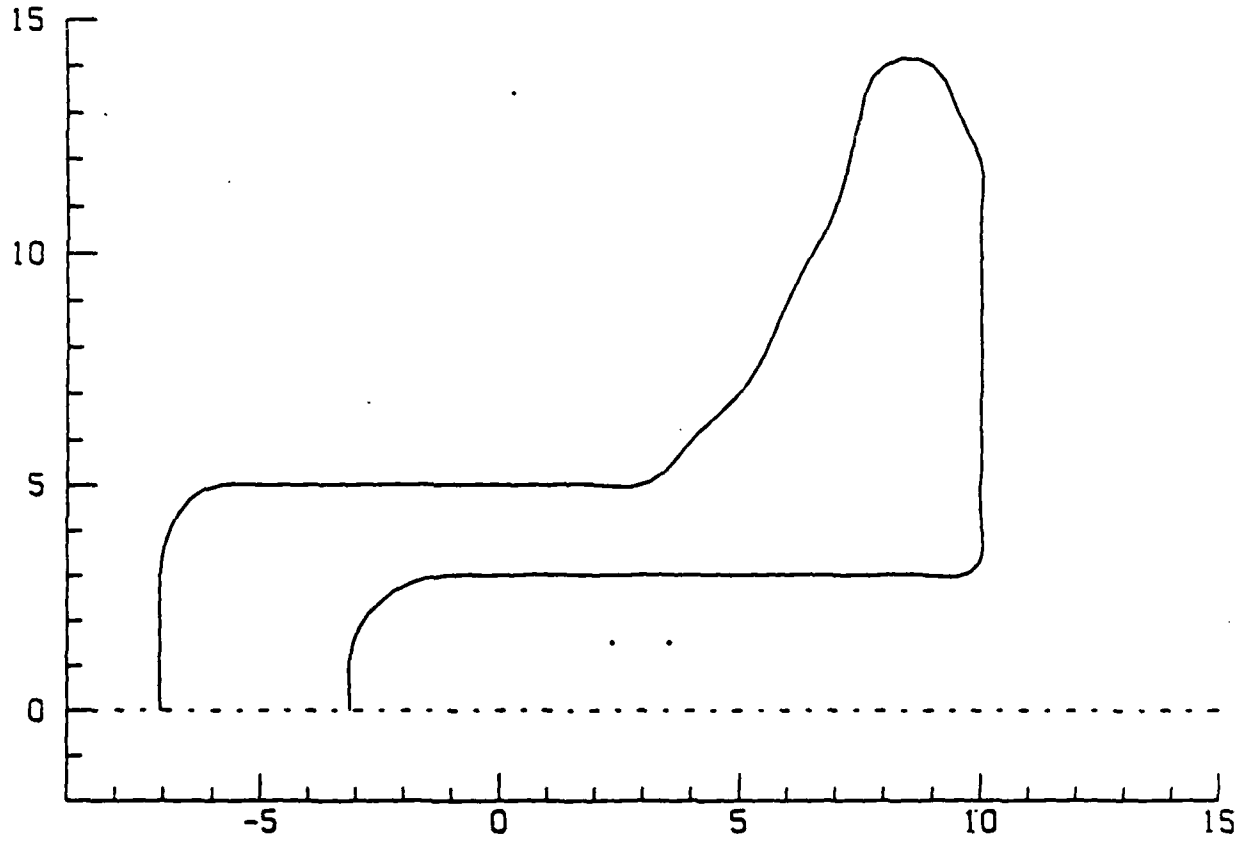

Figure 15

Resampled Waveguide with Test Points in Example 4

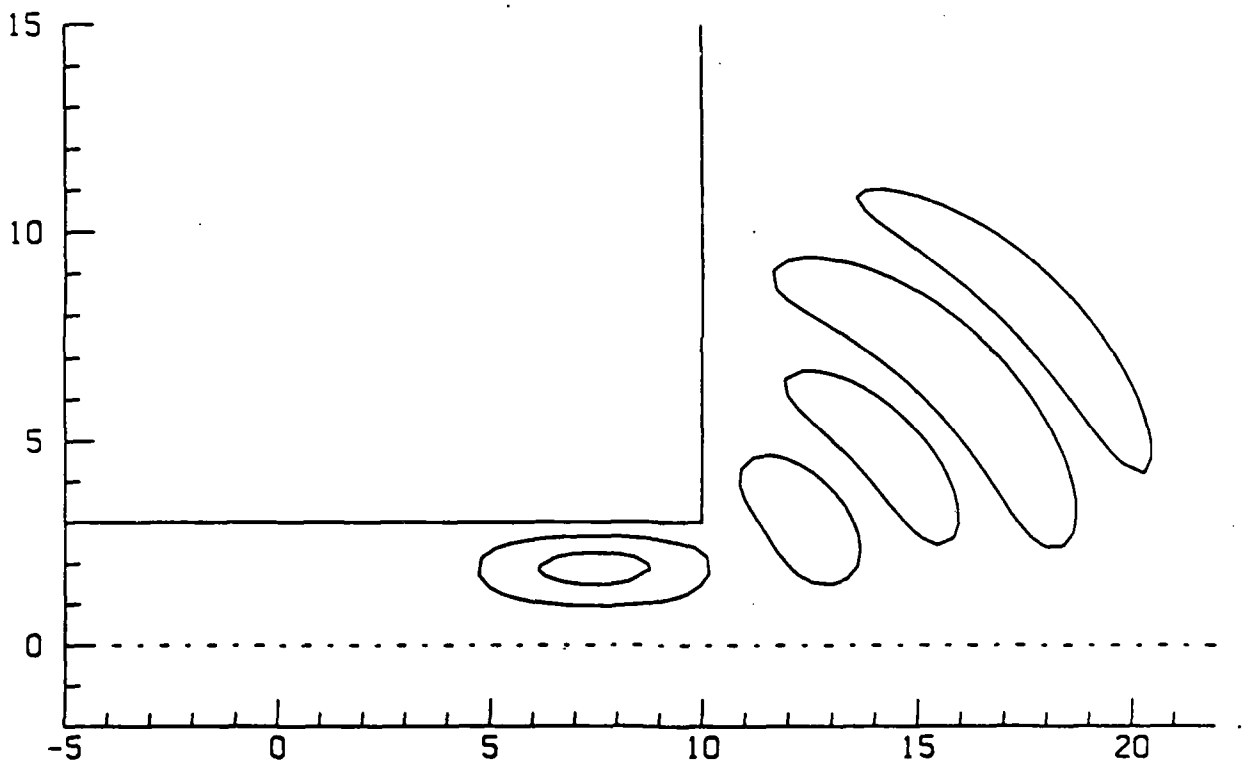

Figure 16

Equipotential Lines of the Real Part of the Solution in Example 4

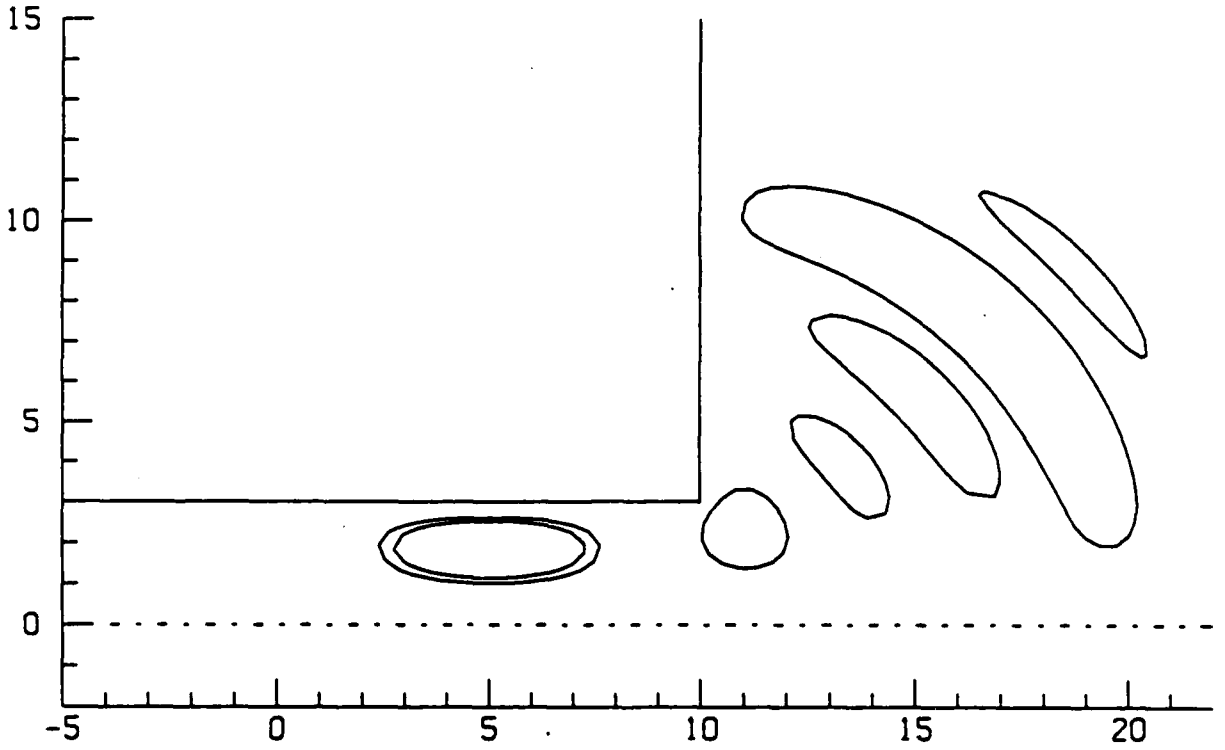

Figure 17

Equipotential Lines of the Imaginary Part of the Solution in Example 4

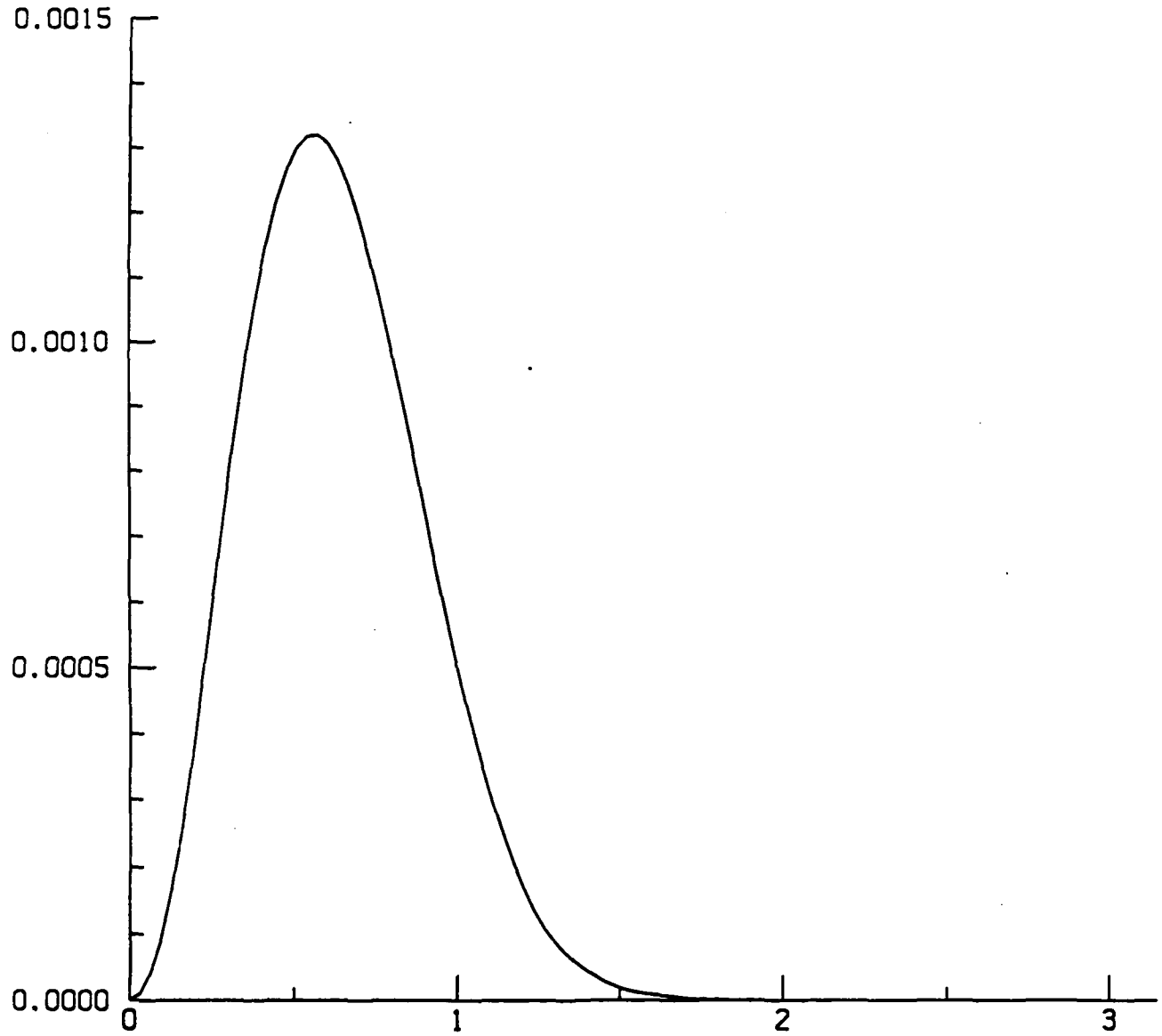

Figure 18

Far-Field Amplitude as a Function of Angle
in Example 4

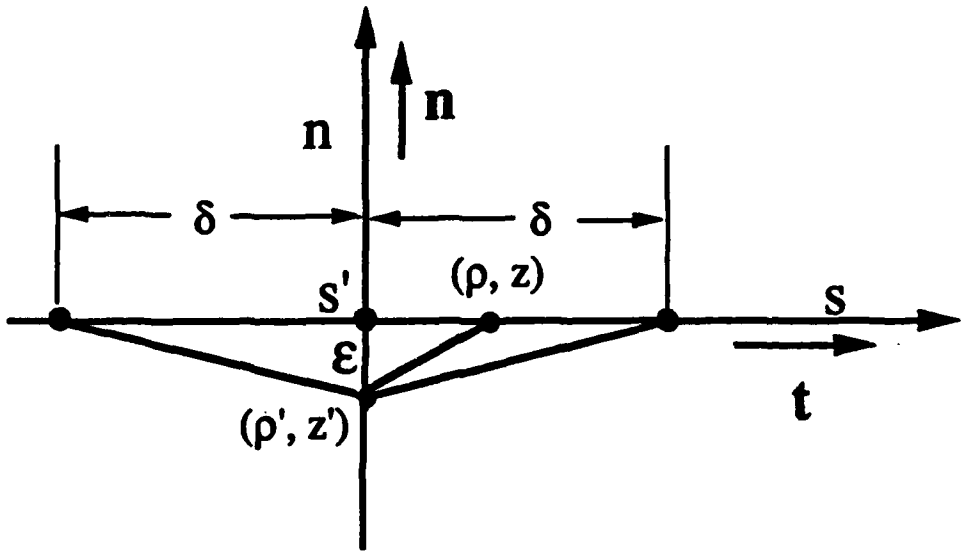

Fig. 19